

**Base-free Aerobic Oxidation of 5-Hydroxymethylfurfural to
2,5-Furandicarboxylic Acid over Pt/C-O-Mg Catalyst**

Journal:	<i>Green Chemistry</i>
Manuscript ID	GC-ART-09-2015-002114.R1
Article Type:	Paper
Date Submitted by the Author:	02-Oct-2015
Complete List of Authors:	Han, Xuewang; East China University of Science and Technology, Geng, Liang; East China University of Science and Technology, Guo, Yong; Research Institute of Petroleum Processing, Sinopec, Jia, Rong; East China University of Science and Technology, Liu, Xiaohui; East China University of Science and Technology, Zhang, Yongguang; Research Institute of Petroleum Processing, Sinopec, Wang, Yanqin; East China University of Science and Technology, Chemistry



Journal Name

ARTICLE

Base-free Aerobic Oxidation of 5-Hydroxymethylfurfural to 2,5-Furandicarboxylic Acid over Pt/C-O-Mg Catalyst

Xuewang Han,^[a] Liang Geng,^[a] Yong Guo,^{*[b]} Rong Jia,^[a] Xiaohui Liu,^[a] Yongguang Zhang^[b] and Yanqin Wang^{*[a]}

Received 00th January 20xx,
Accepted 00th January 20xx

DOI: 10.1039/x0xx00000x

www.rsc.org/

Base-free aerobic oxidation of 5-hydroxymethylfurfural (HMF) to 2,5-furandicarboxylic acid (FDCA) was realized successfully based on the design of a novel Pt/C-O-Mg catalyst. Properties of this catalyst was characterized using TEM, XRD, XPS and temperature-programmed desorption of CO₂. The catalyst had excellent activity and stability, the yield of FDCA reached 97% at optimal conditions (110 °C, O₂ 1.0MPa) and the catalyst was used for ten times with less loss of activity. The excellent activity and stability may come from the formation of C-O-Mg bond, which created new, strong and stable basic sites. Further scaling up the reaction for 20 times, the yield of isolated FDCA reached 74.9% with very high purity (99.5%). This FDCA would be used as the substitute of polymerization monomer for polyethylene terephthalate plastics (PET) synthesis after purification.

Introduction

Nowadays, the conversion of renewable biomass into useful chemicals has attracted much more attention.¹⁻⁵ 5-hydroxymethylfurfural (HMF), a hexose dehydration product, as a key precursor for the synthesis of derivatives has received great attention from the researchers.⁴⁻⁶ 2,5-furandicarboxylic acid (FDCA), formed from HMF, was identified as one of the twelve pivotal sugar-based building blocks which own the largest potential for the production of bio-based chemicals and materials.^{7,8} For example, it could be a green substitute for pure terephthalic acid (PTA) in the production of polyethylene terephthalate plastics (PET).^{9,10} Therefore, the oxidation of biomass-based platform chemical, HMF into FDCA, is of great importance and has been extensively studied in recent decades under a variety of reaction conditions and catalysts.

Generally, the oxidation of HMF to FDCA was carried out either by using stoichiometric oxidants, such as oxygen with highly polluting catalysts (e.g., Pb) in basic conditions, or oxygen with homogeneous metal salts as catalysts (e.g., Co/Mn/Br) in corrosive solvents (e.g., acetic acid), similar to the current production of terephthalic acid.^{11,12} Recently, HMF oxidation was focused on the development of supported noble metal catalysts, including Pt, Au, Pd and Ru, supports were metal oxides or activated carbon.^{5,13-30} In all noble metals, Pt

was the first to be studied, and now is still widely investigated in the HMF oxidation. As early as 1990, Van Bekkum used Pt/Al₂O₃ as the catalyst for HMF oxidation under alkaline conditions.¹⁷ Recently, Davis *et al.*¹⁸ reported the catalytic activity of supported Pt, Pd and Au catalysts at 295 K and high pH in a semi-batch reactor and found that FDCA was formed over Pt/C and Pd/C, but 5-hydroxymethyl-2-furancarboxylic acid (HMFCFA) was formed over Au/C and Au/TiO₂. Besson *et al.*²⁰ reported the oxidation of HMF to FDCA in moderately basic aqueous solutions over activated carbon supported Pt and Pt-Bi catalysts and found Bi can enhance the activity and stability of Pt/C catalyst, as well as the selectivity to FDCA. For industrial process, it is well known that the addition of homogeneous base would increase the risk of reactor corrosion. Therefore, an oxidation reaction of HMF without any homogeneous base would be better fitted the environment friendly industrial application.

In order to avoid using homogeneous base, Gupta *et al.*³¹ developed a hydrotalcite-supported gold nanoparticle catalyst for base-free aerobic oxidation of HMF. The yield of FDCA was close to 100% at 368 K for 7 h. The stability of the catalyst, however, remained a problem due to the leaching of solid base, hydrotalcite into aqueous solution. Wang *et al.*³² also demonstrated the base-free oxidation of HMF into FDCA by using carbon nanotube supported Au-Pd alloy catalyst in water and demonstrated that the carbon nanotube-enhanced adsorption effect and the alloying effect mainly contributed to the realization of the base-free oxidation of HMF to FDCA.

In view of replacing PTA with FDCA in the PET plastics production, the high purity of monomer FDCA is necessary. But FDCA synthesized via HMF oxidation usually contains small amount of 5-formyl-2-furancarboxylic acid (FFCA), an intermediate of HMF oxidation, and it's difficult to be

^a Key Lab for Advanced Materials, Research Institute of Industrial Catalysis, East China University of Science and Technology No. 130 Meilong Road, Shanghai (PR China); Fax: (+ 86) 21-64253824; E-mail: wangyanqin@ecust.edu.cn

^b Research Institute of Petroleum Processing (RIPP), Sinopec; No. 18 Xueyuan Road, P. O. Box 914-12 Beijing 100083, P.R.China; Email: guoyong.ripp@sinopec.com

† Footnotes relating to the title and/or authors should appear here.

Electronic Supplementary Information (ESI) available: See DOI: 10.1039/x0xx00000x

separated from FDCA. So the catalyst with high activity and high selectivity is critical for HMF oxidation. Above all, the exploitation of stable and efficient heterogeneous catalysts for the aerobic oxidation of HMF to FDCA under base-free conditions still remains challenging.

Herein, we designed a novel Pt/C-O-Mg catalyst by coating MgO particles with carbon and then removing free MgO before loading Pt onto carbon surface. The surface of catalyst support is alkaline due to the formation of C-O-Mg bond. Thus prepared Pt/C-O-Mg catalyst exhibits excellent selectivity and stability, the yield of FDCA reached 97% and can be reused for 10 times with less deactivation. Furthermore, when this catalyst was used in larger scale, the isolated yield of FDCA reached 74.9%, retaining its catalytic performance, and crystalline FDCA was obtained with the purity as high as 99.5%.

Experimental Section

Catalyst preparation

Synthesis of MgO-C support: 6 g of commercial light MgO, 9 g of resorcinol and 20 mL of H₂O were mixed in a 100 mL flask and stirred for 30 min. Afterwards, the mixture was sealed into an autoclave and put into an oven at 180 °C for 24 h for hydrothermal treatment and got a brown solid. The obtained brown solid was filtered and washed with deionized water until the filtrate was colourless and then dried at 60 °C overnight. Then carbonation process was carried out in N₂ flow at 30 cm³ min⁻¹ at 800 °C and hold for 3 h. Thus prepared material was denoted as MgO-C. The MgO-C sample was further treated by excess HCl (1 mol L⁻¹) at room temperature for 24 h to remove the free MgO and denoted as C-O-Mg.

Synthesis of Pt/C-O-Mg catalyst: Platinum was loaded by impregnation with an aqueous solution of H₂PtCl₆ followed by reduction. An aqueous solution of H₂PtCl₆ containing the required amount of Pt was added dropwise under stirring to an aqueous suspension of C-O-Mg. After that, the mixture was ultrasonically treated for 0.5 h to ensure the solid being uniformly dispersed. Then excess amount of NaBH₄ was slowly added to the mixture with stirring under room temperature. The solid phase were finally separated by filtration and washed with deionized water for several times, and then dried under vacuum at 60 °C over night. A commercial Pt/C catalyst was purchased from J & K Co. Ltd (Beijing, China) to be the control sample, and denoted as Pt/C-J&K.

As a contrast, HTC catalysts was also synthesized by hydrothermal method, using glucose and resorcinol (mass ratio is 1:1) as carbon source. Here glucose was used as co-carbon source because resorcinol itself cannot form carbon material. The next step is the same as that of synthesis of MgO-C. Similarly, the HTC sample was further treated by excess HCl (1 mol L⁻¹) at room temperature for 24 h, and denoted as HTC-HCl. 5 wt% Platinum was loaded by impregnation on the HTC and HTC-HCl catalysts and denoted as Pt/HTC and Pt/HTC-HCl, respectively.

Catalyst characterization

The synthesized catalysts were fully characterized by the following techniques: Powder X-ray diffraction (XRD) patterns were collected in the θ -2 θ mode using a Bruker D8 Focus diffractometer (CuK α 1 radiation, $k=1.5406$ Å), operated at 40 kV and 40 mA with scattering angles (2θ) of 8–60°.

X-ray photoelectron spectroscopy (XPS) was performed using a Thermo ESCA LAB-250 spectrometer with monochromatic Al K α radiation, and the XPS results were calibrated using the C 1s peak at 284.8 eV. XPS Peak 4.1 was employed to deconvolve the Pt 4f, C 1s and O 1s peaks using the Shirley-type baseline and an iterative least-squared optimization algorithm.

Nitrogen sorption isotherms were measured at 77 K with a NOVA 4200e sorption analyzer. Before the measurements, the samples were degassed at 373 K in vacuum for 8 h. The Brunauer-Emmett-Teller (BET) method was utilized to calculate the apparent surface area.

Temperature programmed desorption of carbon dioxide as probe molecule (CO₂-TPD) was carried out on Micrometrics AutoChem 2920 equipped with mass spectrometry using quadruple spectrometer (MS OmniStar). 100 mg of catalyst was placed in quartz sample tube. Before TPD experiments the catalysts were outgassed at 500 °C for 2 h in a flow of helium. Subsequently the catalysts were cooled down to 50 °C and treated with a CO₂ flow for 60 min. Weak adsorbed CO₂ was removed by flushing with He at 50 °C for 60 min. The desorption of CO₂ was measured by heating the catalyst from 50 °C to 600 °C at a heating rate of 10 °C/min in He flow. The desorbed products were analyzed by mass spectrometry. The number of basic sites was calculated from the CO₂ peaks (the molecular ion, $m/z = 44$).

Scanning electronic microscope (SEM) images were obtained from JEOL JSM-63602V and Hitachi S-3400N microscope operated at 5 kV or 15 kV. Transmission electron microscopy (TEM) images were recorded on a FEI TECNAI G2 F20 s-TWIN instrument, and the electron beam accelerating voltage was 200 kV. Chemical analysis of the samples was performed by using inductively coupled plasma atomic emission spectrometry (ICP-AES).

Reaction procedure and product analysis

The oxidation reaction of HMF was performed in a batch-type Teflon-lined stainless-steel autoclave (100 mL), equipped with an internal thermo-controller and pressure gauge. In a typical catalytic experiment, 0.04 g of catalysts, 10 mL of aqueous solution of HMF (0.05 M) were added to a stirred autoclave reactor. Once the system reached the desired temperature (110 °C), the reaction was initiated by vigorous stirring with a magnetic stirrer under 1.0 MPa of oxygen pressure for 12 h.

When the reaction was finished, the mixture was made alkaline by adding a certain amount of sodium hydrate before filtering off the catalyst, followed by analysis using HPLC (Agilent 1200 series, Bio-Rad Aminex HPX-87H column, 300 mm \times 7.8 mm \times 9 μ m). A 0.004 M H₂SO₄ mobile phase was employed as mobile phase at 55 °C with a flow rate of 0.45 mL min⁻¹. The yields of FDCA and intermediate products were

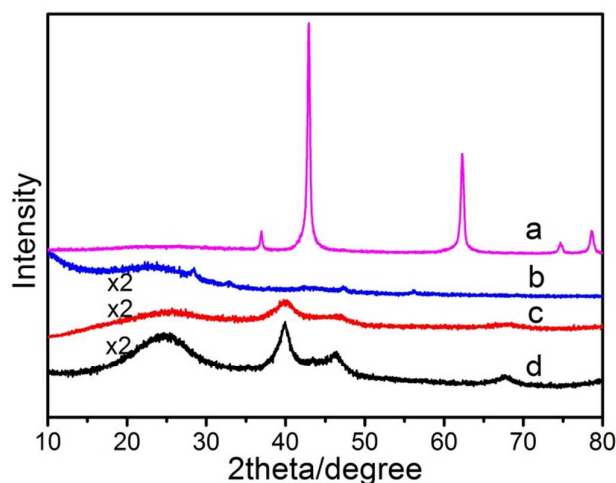


Fig. 1 XRD patterns of (a) MgO-C, (b) C-O-Mg, (c) Pt/C-O-Mg and (d) Pt/C-J&K.

based on conversion of HMF and confirmed by calibration of standard solutions of the reactants and products.

Results and Discussion

Characterization of catalysts

The XRD patterns of MgO-C (carbon-coated MgO), C-O-Mg (HCl washed MgO-C), Pt loaded sample (Pt/C-O-Mg) and commercial Pt/C-J&K are presented in Figure 1. MgO-C (Fig. 1a) exhibits a series of sharp crystalline peaks at 2θ of 37° , 43° , 62.3° , 74.7° and 78.6° , corresponded to (111), (200), (220), (311) and (222) planes of cubic MgO, respectively.³³ Whereas in the XRD pattern of C-O-Mg (Fig. 1b), no any peaks corresponded to cubic MgO are observed, but broad peaks at $20\text{--}30^\circ$ attributed to amorphous carbon (002) plane are obvious, indicating that bulk MgO has been removed successfully by HCl. Pt/C-O-Mg and Pt/C-J&K showed similar XRD patterns (Fig. 1c, d), but the former exhibits broader diffraction peaks of Pt nanoparticles, suggesting the Pt particle size of Pt/C-O-Mg is smaller, about 2.51 nm according to Debye-Scherrer's equation.³⁴ The BET surface area of Pt/C-O-Mg catalyst was $1220\text{ m}^2\text{ g}^{-1}$, while that of Pt/C-J&K was $759\text{ m}^2\text{ g}^{-1}$.

The SEM and TEM image of Pt/C-O-Mg are shown in Fig. 2. SEM image revealed that Pt/C-O-Mg has a folded lamellar morphology which consists of thin plates up to 50–150 nm thick. The highly dispersed Pt nanoparticles on carbon surface are observed from TEM image, a narrow size distribution is obtained, concentrated at 2.5 nm, consistent with the particle size calculated from XRD pattern. Such high dispersion of Pt nanoparticles may contribute to the better catalytic activity of Pt/C-O-Mg in HMF oxidation. In addition, The TEM images and the corresponding Pt particle size distribution of the Pt/C-J&K and Pt/HTC-HCl catalysts are shown in Figure S1. The histogram of the Pt particle size distribution shows that most of the Pt particles are distributed in the range of 2.0–3.5 nm.

The atomic emission spectroscopy of Pt/C-O-Mg shows that there are 0.18% Mg and 5.3% Pt, which proved that not all of

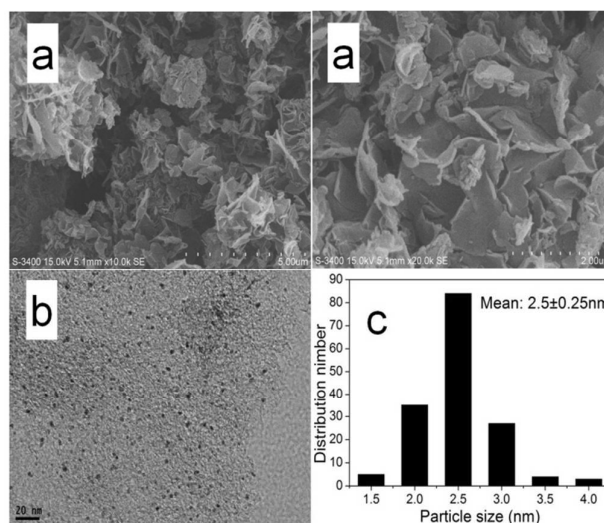


Fig. 2 SEM (a) and TEM (b) images of Pt/C-O-Mg catalyst and the corresponding particle size distribution (c).

MgO was removed by HCl. The residual magnesium may be contributed to the alkalinity of carbon support and favors the HMF oxidation into FDCA. In order to investigate the surface composition (include Pt, C, O and Mg) of Pt/C-O-Mg, XPS analysis was also carried out. The Pt 4f spectra of Pt/C-O-Mg displays two doublets from the spin-orbital splitting of the $4f_{7/2}$ and $4f_{5/2}$ with Pt (0) and Pt (II) states, as shown in Figure 3a. In general, the positions of the Pt XPS signals are influenced by the valence state of Pt, e.g. the binding energy for bivalent Pt is usually higher than that for metallic Pt. These doublets contain a low energy band centered at 70.9 eV and high energy band at 74.5 eV, indicating that the Pt is present in its metallic state Pt (0), which is considered to play a key role in HMF oxidation.¹⁹ In order to identify the higher oxidation states of Pt, the spectrum has been curve fitted and the smaller doublets are detected at higher binding energy positions, i.e., at 73.3 and 76.7 eV, respectively, and reveal the existence of Pt (II) state (PtO species) in the catalyst.³⁴ The percentage of these two species (Pt (0) and Pt (II)) is 70.4% and 29.6% respectively.

The XPS spectra of Pt/C-O-Mg catalyst showed typical asymmetric peaks in the C 1s region and typical symmetric peaks in the O1s region. The deconvolution of the C 1s spectra yielded four peaks:^{36,37} peak 1 (284.6 eV), graphitized carbon; peak 2 (286.1 eV), carbon in phenolic, alcohol or ether groups; peak 3 (289.5 eV), carbon in carboxyl or ester groups. Similarly, the deconvolution of the O 1s spectra yielded the following four peaks:^{38,39} peak 1 (531.4 eV), carbonyl oxygen of quinines; peak 2 (532.5 eV), carbonyl oxygen atoms in esters, anhydrides and oxygen atoms in hydroxyl groups; peak 3 (533.6 eV), non-carbonyl (ether-type) oxygen atoms in esters and anhydrides; and peak 4 (535.4 eV), adsorbed water and/or oxygen. But no signal of Mg (1303.3 eV) was observed, maybe due to its low content. Figure 3 show typical XPS results together with fitted Pt 4f, C 1s, O 1s and Mg 1s peaks. Table 1

summarizes the binding energies (eV) and relative intensities (%) of the Pt 4f, C

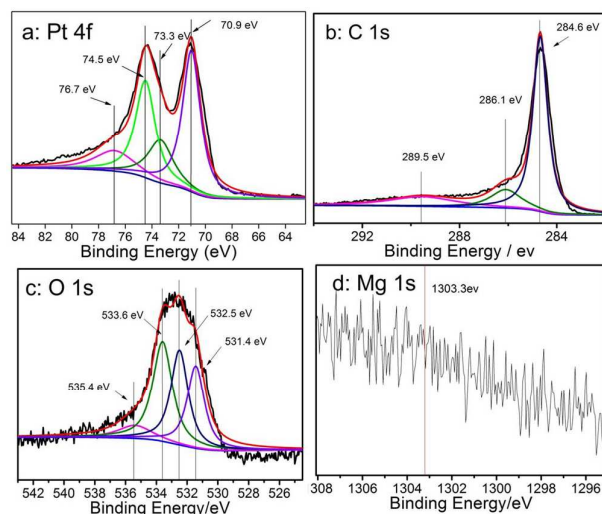


Fig. 3 XPS spectra of Pt/C-O-Mg catalysts and fitting curves: (a) Pt 4f, (b) C 1s and (c) O 1s, (d) Mg 1s.

Table 1 The binding energies and relative intensities of different Pt, C and O species as observed from the respective Pt 4f, C 1s and O 1s spectrum of Pt/C-O-Mg catalyst

Ele.	Species	Binding energy (eV)	Relative intensity (%)
Pt 4f	Pt (0)	70.9	70.4
	Pt (II)	73.3	29.6
C 1s	C-C	284.6	68.3
	C-O	286.1	14.8
	C=O	289.5	16.9
O 1s	OH- or C=O from quinonyl	531.4	26.1
	C=O	532.5	30.2
	C-O	533.6	35.8
	H ₂ O and/or O ₂	535.4	7.9

1s and O 1s peaks.

The alkalinity of Pt/C-O-Mg was confirmed via CO₂-TPD and the result is present in Fig. 4. Following the desorption peak of weakly adsorbed CO₂ at 81 °C, two kinds of basic sites are detected, located at 135 and 251 °C, respectively. Meanwhile, commercial catalyst Pt/C-J&K shows only one weak CO₂ desorption peak at 81 °C, and its total CO₂ uptake is much lower. It indicated that involving MgO in catalyst preparation introduced new basic site to Pt/C catalyst, and made it a sort of solid base. To identify these new basic sites, CO₂-TPD of pure magnesium oxide was also carried out. There are two desorption peaks at 92 and 168 °C, respectively (Fig. 4a), suggesting the existence of weak basic sites. It is interesting to note that Pt/C-O-Mg exhibited a new kind of stronger basic site at 251 °C, compared with pure MgO, and may be

attributed to the formation of C-O-Mg bond. Basic sites could accelerate the activation of hydroxyl and the formation of intermediate hemiacetal in base-free aerobic oxidation

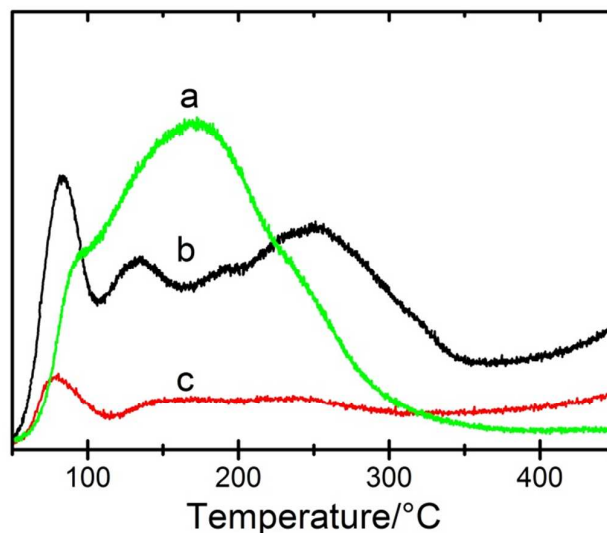


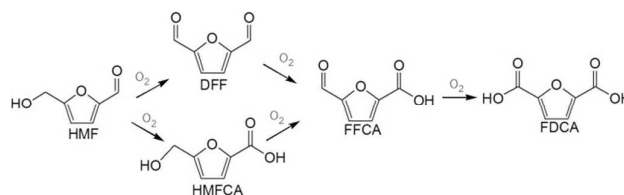
Fig. 4 CO₂-TPD of (a) MgO, (b) Pt/C-O-Mg and (c) Pt/C-J&K.

reaction of alcohols.³¹ Thus, this kind of Pt/C-O-Mg catalyst would be a good catalyst for HMF oxidation in base-free conditions.

Catalyst activity

The aerobic oxidation of HMF to FDCA over Pt catalysts usually follows the pathway displayed in Scheme 1. The hydroxymethyl group of HMF was quickly converted into formyl group of DFF via the activation of hydroxyl owing to activation of Pt active sites and basic sites. Then, one of formyl groups of DFF was subsequently oxidized to carboxyl group to yield FFCA via the formation of the intermediate hemiacetal due to the effect of the basic sites. Finally, the second formyl was turned into carboxyl group and the final product FDCA was formed via intermediate hemiacetal, which is usually the rate-controlling step in the overall reaction.^{18,31}

A typical aerobic oxidation of HMF over Pt/C-O-Mg was carried out at 110 °C, under 1.0 MPa O₂. Without homogeneous base, such as NaOH, Na₂CO₃ or NaHCO₃, the feedstock of HMF was also completely converted and the yield of FDCA reached 97%. As shown in Figure 5a, in a short reaction time, the intermediates, DFF and FFCA were detected. The initially formed DFF could be quickly transformed into FFCA, but the further oxidation of FFCA to FDCA is much slower, appears the rate-controlling step, which is consistent with the reported profile of Pt catalyzed HMF oxidation.¹⁹



Scheme 1 Reaction pathway for the oxidation of HMF using Pt/C-O-Mg catalyst, HMFCFA is not detected (HMF = 5-Hydroxymethylfurfural, DFF = 2,5-Diformylfuran, HMFCFA = 5-Hydroxymethyl-2-furancarboxylic acid, FFCA = 5-formyl-2-furancarboxylic acid, FDCA = 2,5-Furandicarboxylic acid).

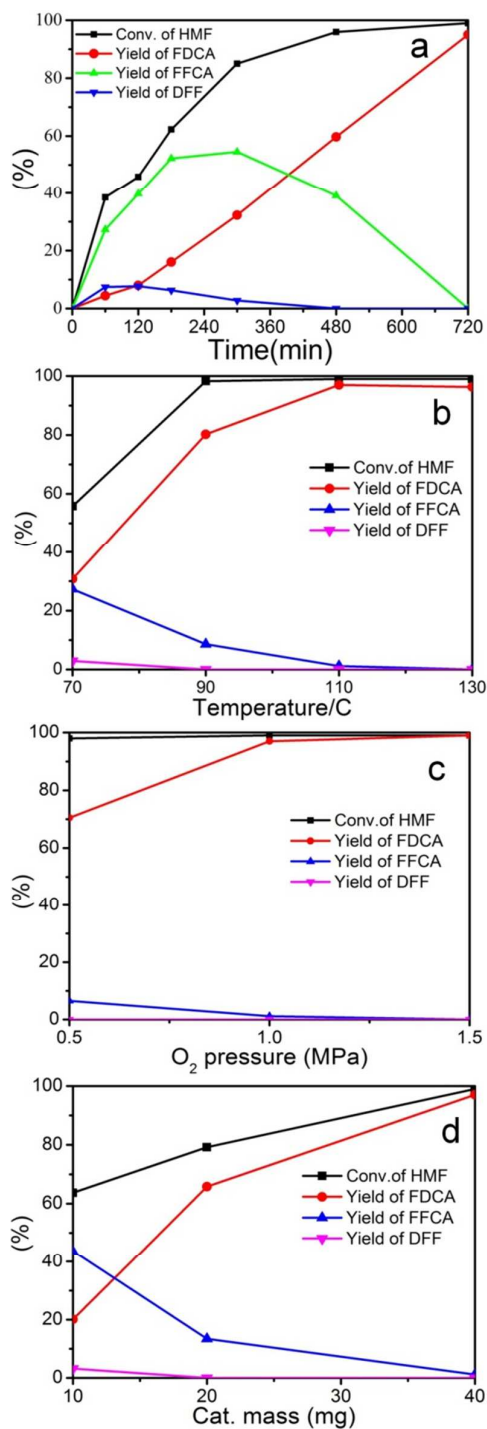


Fig. 5 (a) Time course of HMF oxidation over Pt/C-O-Mg catalyst. Reaction conditions: HMF (0.5 mmol), H₂O (10 ml), Pt/C-O-Mg (0.04 g), molar ratio HMF/Pt = 50, 110 °C, 12 h, O₂ 1.0 MPa; (b) Effect of reaction temperature on HMF oxidation. Reaction conditions: HMF (0.5 mmol), H₂O (10 ml), Pt/C-O-Mg (0.04 g), molar ratio HMF/Pt = 50, 12 h, O₂ 1.0 MPa; (c) Effect of oxygen pressure on HMF oxidation. Reaction conditions:

HMF (0.5 mmol), H₂O (10 ml), Pt/C-O-Mg (0.04 g), molar ratio HMF/Pt = 50, 110 °C, 12 h; (d) Effect of catalyst dosage on HMF oxidation. Reaction conditions: HMF (0.5 mmol), H₂O (10 ml), 110 °C, 12 h, O₂ 1.0 MPa.

The influence of temperature and O₂ pressure in the catalytic conversion of HMF over Pt/C-O-Mg catalyst was investigated and plotted in Figures 5b and 5c, respectively. The conversions of HMF are >99 % in most conditions. With the increase of reaction temperature, the yield of FDCA increased significantly (Fig. 5b), 97 % yield of FDCA was obtained at 110 °C with a small amount of FFCA was detected. At lower pressure (0.5 MPa), the intermediate products were FFCA and DFF, meaning the oxidation process was incomplete. Further increase the reaction pressure to 1.0 and 1.5 MPa, the activity of the Pt/C-O-Mg catalyst increased and a higher FDCA yield was obtained (Fig. 5c). In order to determine the optimum catalyst dosage, a series of Pt/C-O-Mg catalysts with different dosage were and tested for the conversion of HMF (Fig. 5d). As shown in Table 3, the yield of FDCA increased notably when the catalyst dosage increases from 10 to 40 mg.

Effect of the solvent

The aerobic oxidation of HMF was further carried out in a variety of solvents. As shown in Table 3, the solvent showed a remarkable effect on the oxidation of HMF. H₂O with strong polarity was found to be the best solvents, that the HMF conversion and FDCA yield reached over 99% and 97%, respectively (Table 2, Entry 7). HMF conversion around 20% were obtained in CH₃CN and DMSO (dimethyl sulfoxide) (Table 2, Entries 1 and 2), and the yield of FDCA was almost zero. Reactions carried in DMF (dimethylformamide) and GVL (γ -valerolactone) produced high HMF conversion (Table 2, Entries 3 and 4). However, the yield of DFF in GVL was highest than that in other solvents, as most of the DFF could not be oxidized further into FDCA. Higher conversion of HMF was detected in 1,4-Dioxane and MIBK (methyl isobutyl ketone) (Table 2, Entries 5 and 6), but the yield of FDCA was still relatively low compared with entry 7. During the reaction process, parts of the reaction solvents were partially oxidized and HMF was converted to side product, and these were not what we want. Many other researchers reported the effect of solvents on the oxidation reaction. However, most organic solvents cannot effectively promote the reaction of HMF into FDCA, except methanol, may be due to it is a protonic solvent. Parts of the results are shown in Table S2. These results indicated that water was a superior solvent for the aerobic oxidation of HMF into FDCA. Thus, the oxidation of HMF using water as a green solvent is very appealing because water is cheaper and environmental friendly.

Activity of different catalysts

Under the optimal conditions, the yield of FDCA using commercial catalyst Pt/C-J&K was only 62.8%, and around 37% of HMF was converted to side product, humans, etc (Table 3, Entry 3). Whereas HMF could be almost selectively converted to FDCA over Pt/C-O-Mg, indicated that Pt/C-O-Mg catalyst could favor HMF oxidation through extra basic site, hence exhibit higher activity than commercial Pt/C in the base-free

condition. We also studied the activity of Pt/HTC catalyst, made from resorcinol with and without the treatment with HCl, but the selectivity to FDCA was lower (Table S1).

Table 2. Catalytic results of HMF oxidation in different solvent under base-free conditions.

Entry	Solvent.	Conv.(%)	$Y_{\text{FDCA}}(\%)$	$Y_{\text{FFCA}}(\%)$	$Y_{\text{DFE}}(\%)$
1	CH ₃ CN	16.2	0	0.6	6.0
2	DMSO	21.5	0.8	7.0	9.0
3	DMF	43.8	1.7	11.9	3.3
4	GVL	63.3	0	8.3	35.9
5	1,4-Dioxane	98.2	6.2	5.9	0
6	MIBK	98.4	19.1	10.5	3.0
7	H ₂ O	>99	97.0	1.2	0

Reaction conditions: Cat. Pt/C-O-Mg (0.04 g), HMF (0.5 mmol), Solv. (10 mL), 110 °C, 12 h, O₂ 1.0MPa.

Table 3. Catalytic results of HMF oxidation in water using different catalysts under base-free conditions.

Entry	Cata.	Conv. (%)	$Y_{\text{FDCA}}(\%)$	$Y_{\text{FFCA}}(\%)$	$Y_{\text{DFE}}(\%)$
1	Pt/MgO	>99	95.5	0	0
2	Pt/MgO-C	>99	99.2	0	0
3	Pt/C-J&K	>99	62.8	0.3	0
4	Pt/C-O-Mg	>99	97.0	1.2	0
5	Pt/HTC-HCl	>99	58.9	26.3	0

Reaction conditions: HMF (0.5 mmol), H₂O (10 ml), catalysts (0.04 g), molar ratio HMF/Pt = 50, 110 °C, 12 h, O₂ 1.0 MPa.

Furthermore, Pt nanoparticles loaded on pure MgO and MgO-C composite are both applied in HMF oxidation reaction (Table 3, Entries 1 and 2). Their FDCA yields reached as high as 95.5% and 99.2%, respectively, because the supports contain a large amount of bulky MgO as solid base. However, bulky MgO is a kind of unstable support in aqueous solvent, which will be dissolved gradually in aqueous solution and lost its activity.¹⁹

Catalyst stability and reusability

While the stability and recyclability of catalyst is of great importance for its application prospect of industrialization. Therefore, we studied the stability of the Pt/MgO-C catalyst (Fig. 6a). This catalyst was simply reused by centrifugation, water washing and vacuum drying at 60 °C without adding fresh catalyst. Experimental results show that the catalytic activity and dosage of the catalyst decreased obviously with the increase of the cycle numbers. After reaction, the catalyst mass decreased from 40 mg to 23 mg, because a large amount of MgO was dissolved.

Similarly, the Pt/C-O-Mg catalyst was reused for 10 times to investigate its stability (Fig. 6b). The catalytic performance of each run is shown and found no obvious deactivation

happened. HMF was completely converted in all runs, and the FDCA yield was generally stable at around 95% with less decrease (from 97 to 95%), perhaps due to the oxidation of Pt nanoparticles, aggregation of Pt nanoparticles and the leaching

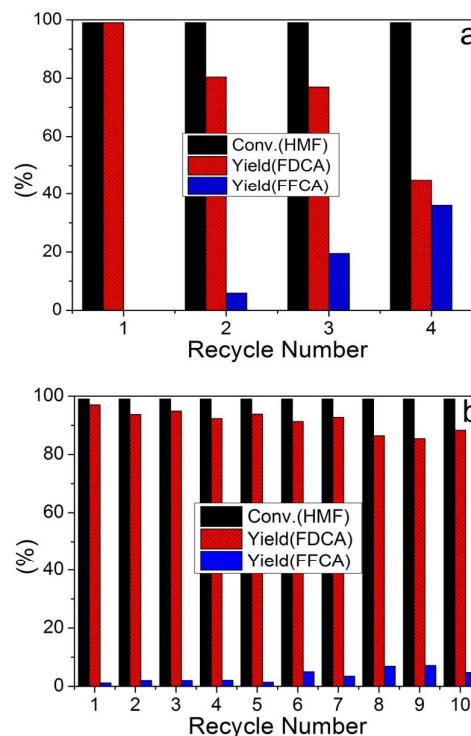


Fig. 6 Reusabilities of Pt/MgO-C (a) and Pt/C-O-Mg (b) catalysts without homogeneous base in the transformation of HMF to FDCA. Reaction conditions: HMF (0.5 mmol), H₂O (10 ml), catalyst (0.04 g), molar ratio HMF/Pt = 50, 110 °C, 12 h, O₂ 1.0 MPa.

of platinum. Given the mild reaction conditions, there was only a little growth or aggregation of Pt nanoparticles on used catalyst based on TEM observation and the histogram of the Pt nanoparticle size distribution shown in Figure S2. XPS spectrum shows that the electronic states of Pt had no obvious changes (Fig. S3) after reaction, while inductively coupled plasma atomic emission spectroscopy (ICP-AES) analysis shows the slight leaching of Pt happened and the Pt loadings of the fresh and used catalyst were 5.3 and 4.7 wt %, respectively, indicating the leaching of Pt may be leading to the slight

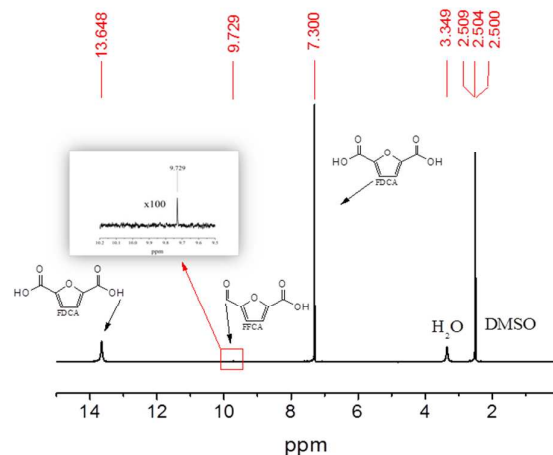


Fig. 7 ^1H -NMR spectrum of isolated FDCA product. Reaction conditions: Pt/C-O-Mg 0.8g, HMF 5.04g, molar ratio HMF/Pt = 200, H_2O 200mL, 2.0 MPa O_2 , 130 $^\circ\text{C}$, 24 h.

indicating the leaching of Pt may be leading to the slight decrease of FDCA yield. In addition to, a small amount loss of the catalyst during centrifuged separation was also a reason for the slightly decrease of catalyst activity. Therefore, Pt/C-O-Mg is an excellent catalyst for HMF oxidation in base-free conditions in view of both activity and stability.

Study on scale-up experiment

In order to verify the excellent catalytic activity of the catalyst, the excellent activity of Pt/C-O-Mg has also been demonstrated in larger reaction scale. The yields of FDCA and FFCA reached 91.6% and 6.1%, respectively, with 99% HMF conversion, and the yield of isolated FDCA reached 74.9% when the initial concentration of HMF and total reaction volume increased 4 and 20 times, respectively (molar ratio HMF/Pt = 200, reaction conditions are shown in Fig. 7). Upon the reaction came to a close, FDCA would crystallize and precipitate. Following dissolving it by NaOH and separate the solid catalyst by centrifugation, the liquid phase was acidified by concentrated HCl to precipitate the crystalline FDCA. The pure FDCA were decolorized by activated carbon and the white product was obtained, its photo is shown in Supporting Information. Analyzed via HPLC and ^1H NMR, the purity of obtained FDCA is over 99.5% (^1H NMR pattern is shown in Fig. 7). The pure FDCA could be readily used as monomer precursor of polyethylene furandicarboxylate (PEF) production.

Conclusions

Above all, we synthesized Pt/C-O-Mg catalyst for HMF aerobic oxidation to FDCA in water under base-free conditions, the support showed strong alkalinity whose support showed strong alkalinity and thus could play as a kind of solid base to favor the reaction. The catalyst demonstrated higher activity and excellent stability than commercial Pt/C catalyst and other catalysts we prepared. The excellent activity of the catalyst has also been demonstrated in larger scale reaction, and the pure FDCA product could be obtained.

Acknowledgements

This project was financially supported by the National Natural Science Foundation of China (no. 21273071 and 21403065) and the Fundamental Research Funds for the Central Universities.

References

- 1 P. Gallezot, *Chem. Soc. Rev.*, 2012, **41**, 1538-1558.
- 2 A. Corma, S. Iborra and A. Velty, *Chem. Rev.*, 2007, **107**, 2411-2502.
- 3 J. B. Binder, R. T. Raines, *J. Am. Chem. Soc.*, 2009, **131**, 1979-1985.
- 4 X. Tong, Y. Ma and Y. Li, *Appl. Catal. A: Gen.*, 2010, **385**, 1-13.
- 5 M. Besson, P. Gallezot and C. Pinel, *Chem. Rev.*, 2013, **114**, 1827-1870.
- 6 S. Siankevich, Z. Fei, R. Scopelliti, G. Laurency, S. Katsyuba, N. Yan and P. J. Dyson, *ChemSusChem*, 2014, **7**, 1647-1654.
- 7 T. Werpy, G. Petersen, A. Aden, J. Bozell, J. Holladay, J. White, A. Manheim, D. Eliot, L. Lasure and S. Jones, Top value added chemicals from biomass. Volume 1-Results of screening for potential candidates from sugars and synthesis gas. Pacific Northwest National Laboratory (PNNL) and National Renewable Energy Laboratory (NREL). 2004, 1-477.
- 8 J. N. Chheda, G. W. Huber and J. A. Dumesic, *Angew. Chem., Int. Ed.* 2007, **46**, 7164-7183.
- 9 A. J. J. E. Eerhart, A. P. C. Faaij and M. K. Patel, *Energy Environ. Sci.*, 2012, **5**, 6407-6422.
- 10 E. De Jong, M. A. Dam, L. Sipos and G. J. M. Gruter, *Biobased monomers, polymers, and materials Vol. 1105* (Eds.: P. B. Smith, R. A. Gross) ACS Symposium Series, Washington 2012, pp. 1-13.
- 11 W. Partenheimer, V. V. Grushin, *Adv. Syn. Catal.*, 2001, **343**, 102-111.
- 12 P. Verdegue, N. Merat and A. J. Gaset, *Mol. Catal.*, 1993, **85**, 327-344.
- 13 S. E. Davis, B. N. Zope and R. J. Davis, *Green Chem.*, 2012, **14**, 143-147.
- 14 H. Ait Rass, N. Essayem and M. Besson, *ChemSusChem*, 2015, **8**, 1206-1217.
- 15 S. Siankevich, G. Savoglidis, Z. Fei, G. Laurency, D. T. L. Alexander, N. Yan and P. J. Dyson, *J. Catal.*, 2014, **315**, 67-74.
- 16 S. E. Davis, M. S. Ide and R. J. Davis, *Green Chem.*, 2013, **15**, 17-45.
- 17 P. Vinke, H. H. van Dam and H. van Bekkum, *Stud. Surf. Sci. Catal.*, 1990, **55**, 147-158.
- 18 S. E. Davis, L. R. Houk, E. C. Tamargo, A. K. Datye and R. J. Davis, *Catal. Today*, 2011, **160**, 55-60.
- 19 Y. Y. Gorbanev, S. Kegnaes and A. Riisager, *Top. in Catal.*, 2011, **54**, 1318-1324.
- 20 H. A. Rass, N. Essayem and M. Besson, *Green Chem.*, 2013, **15**, 2240-2251.
- 21 O. Casanova, S. Iborra and A. Corma, *ChemSusChem*, 2009, **2**, 1138-1144.
- 22 J. Cai, H. Ma, J. Zhang, Q. Song, Z. Du, Y. Huang and J. Xu, *Chem.-Euro. J.*, 2013, **19**, 14215-14223.
- 23 S. Albonetti, A. Lolli, V. Morandi, A. Migliori, C. Lucarelli and F. Cavani, *Appl. Catal. B: Environ.*, 2015, **163**, 520-530.
- 24 A. Villa, M. Schiavoni, S. Campisi, G. M. Veith and L. Prati, *ChemSusChem*, 2013, **6**, 609-612.

- 25 Y. Y. Gorbanev, S. K. Klitgaard, J. M. Woodley, C. H. Christensen and A. Riisager, *ChemSusChem*, 2009, **2**, 672-675.
- 26 T. Mallat, A. Baiker, *Chem. Rev.* 2004, **104**, 3037-3058.
- 27 T. Liu, Y. S. Ren and Z. H. Zhang, *Green Chem.*, 2015, **17**, 1610-1617.
- 28 Z. Z. Miao, T. X. Wu, J. W. Li, T. Yi, Y. B. Zhang and X. G. Yang, *RSC Advances*, 2015, **5**, 19823-19829.
- 29 Z. Z. Miao, Y. B. Zhang, X. G. Pan, T. X. Wu, B. Zhang, J. W. Li, T. Yi, Z. D. Zhang and X. G. Yang, *Catal. Sci. Technol.*, 2015, **5**, 1314-1322.
- 30 Z. H. Zhang, J. D. Zhen, B. Liu, K. L. Lv and K. J. Deng, *Green Chem.*, 2015, **17**, 1308-1317.
- 31 N. K. Gupta, S. Nishimura, A. Takagaki and K. Ebitani, *Green Chem.*, 2011, **13**, 824-827; L. Ardemani, G. Cibin, A. J. Dent, M. A. Isaacs, G. Kyriakou, A. F. Lee, K. Wilson, *Chem. Sci.*, 2015, **6**, 4940-4945; A. Abad, A. Corma, H. Garcia, *Chem.-Eur. J.*, 2008, **14**, 212.
- 32 X. Wan, C. Zhou, J. Chen, W. Deng, Q. Zhang, Y. Yang and Y. Wang, *ACS Catal.*, 2014, **4**, 2175-2185.
- 33 M. A. Aramendía, J. A. Benítez, V. Borau, C. Jiménez, J. M. Marinas, J. R. Ruiz and F. Urbano, *Langmuir*, 1999, **15**, 1192-1197.
- 34 L. S. Birks, H. Friedman, *J. Appl. Phys.*, 1946, **17**, 687-692.
- 35 J. F. Moulder, W. F. Stickle, P. E. Sobol, K. D. Bomben, *Handbook of X-ray photoelectron spectroscopy*. Chastain. J. Ed., Perkin-Elmer Corporation. 1995, pp. 253 - 265.
- 36 Z. R. Yue, W. Jiang, L. Wang, S. D. Gardner and C. U. Pittman, *Carbon*, 1999, **37**, 1785-1796.
- 37 P. V. Lakshminarayanan, H. Toghiani and C. U. Pittman, *Carbon*, 2004, **42**, 2433-2442.
- 38 U. Zielke, K. J. Hüttinger and W. P. Hoffman, *Carbon*, 1996, **34**, 983-998.
- 39 L. She, J. Li, Y. Wan, X. Yao, B. Tu and D. Zhao, *J. Mater. Chem.*, 2011, **21**, 795-800.